

Theory of Nonlinear Diffusion with a Physical Gapped Mode

Navid Abbasi*


School of Nuclear Science and Technology, Lanzhou University, 222 South Tianshui Road, Lanzhou 730000, China

Matthias Kaminski[†]

Department of Physics and Astronomy, University of Alabama, Tuscaloosa, Alabama 35487, USA

Omid Tavakol[‡]

Department of Physics, University of Toronto, Toronto, Ontario M5S 1A7, Canada

 (Received 6 March 2023; revised 18 February 2024; accepted 4 March 2024; published 29 March 2024)

In a system with one conserved charge the charge diffusion is modified by nonlinear self-interactions within an effective field theory (EFT) of diffusive fluctuations. We include the slowest ultraviolet (UV) mode, constructing a UV-regulated EFT. The relaxation time of this UV mode is protected from renormalization, as supported by experimental data in a bad metal system. Furthermore, the retarded density-density Green's function acquires four branch points, eventually increasing the range of applicability. We discuss the fate of long time tails as well as implications for the quark gluon plasma.

DOI: [10.1103/PhysRevLett.132.131602](https://doi.org/10.1103/PhysRevLett.132.131602)

Introduction.—In a system with a single conservation law, the late-time dynamics is universally described by hydrodynamic diffusion of the associated conserved charge. In the effective field theory (EFT) approach to hydrodynamics [1–4], the linear diffusion equation is derived as the equation of motion from a classical quadratic effective action. If the diffusion constant depends on the transported density, then this equation becomes nonlinear [5]. This is caused by the (self-)interactions encoded in the corresponding effective action, eventually affecting the correlation functions [6,7].

The onset of diffusion in a system can be characterized by the *relaxation time* τ , the timescale of the relaxation of that nonconserved quantity which relaxes slowest. In the limiting case $\tau = 0$, the interacting EFT of hydrodynamics predicts long time tails [10] and large renormalization effects for the transport coefficients [11]. In this limit, which corresponds to the instantaneous response of the current to the source, hydrodynamic equations fail to satisfy the commutation sum rules [12]. Therefore, a finite relaxation rate $1/\tau$ has to be considered to regulate the theory of diffusion discussed above. Such a relaxation rate has been recently measured in ultracold gas of ${}^6\text{Li}$ in a two-dimensional lattice, an example of a “bad metal,” as the testing ground for the Fermi-Hubbard model [13].

The aforementioned relaxation time τ characterizes the timescale of the establishment of local thermal equilibrium in a U(1) static system [14,15]. Since the local equilibration cannot happen arbitrarily quickly, it is expected for τ to be subject to a lower bound [14]. It is then important to understand how this bound is affected by fluctuations. This can be investigated via studying the effect of self-interactions in the EFT framework, in particular, the renormalization effects. In fact, we need to increase the EFT cutoff of [6,7] to include at least the slowest UV mode. Indeed, this leads us to derive, for the first time, a UV-regulated theory of nonlinear diffusion with a physical gapped mode.

Another motivation manifests itself in the long time tails. It is well known that in a many body system, at late times, the autocorrelation functions feature long time tails [18,19]. Now the question is what happens to these tails when the local thermalization is not instantaneous. Does the thermalization occur exponentially fast [20]? If not, would it possibly lead to a longer tail for correlation functions, thereby delaying the global thermalization?

Keeping these questions in mind, in the following, we construct the EFT including fluctuations for a self-interacting system with a single conserved density together with a single gapped mode; the longest-lived gapped mode, acting as a UV-regulator for the EFT. Our effective action is consistent with the general framework of [1], however, derived through the traditional Martin-Siggia-Rose (MSR) formalism [22]. Explicitly calculating the one-loop retarded density-density Green's function, we discuss how the renormalization of the diffusion constant at $\tau = 0$, performed in [6,7], is affected by the gapped mode. In particular, we discuss the renormalization of the relaxation

Published by the American Physical Society under the terms of the [Creative Commons Attribution 4.0 International license](https://creativecommons.org/licenses/by/4.0/). Further distribution of this work must maintain attribution to the author(s) and the published article's title, journal citation, and DOI. Funded by SCOAP³.

time which was not included in [6,7]. The renormalized Green's functions then will be used to study the effect of the gapped mode on long time tails. We conclude by discussing the application of our results to a bad metal [13], expanding quark gluon plasma (QGP) and also to the QGP droplet near the QCD critical point. Natural units, $k_B = 1 = \hbar$, are implied.

Setup.—Beginning in the absence of interactions, we consider a U(1) conserved charge with a nonrelativistic nonconserved current as follows:

$$\partial_t n + \nabla \cdot \mathbf{J} = 0, \quad \tau \partial_t \mathbf{J} + \mathbf{J} + D \nabla n = 0, \quad (1)$$

with D being a constant. For finite τ , the combination of the two equations in (1) leads to

$$\tau \partial_t^2 n + \partial_t n - D \nabla^2 n = 0. \quad (2)$$

This equation describes the dynamics of the diffusive density mode together with a gapped mode

$$\omega_{1,2} = -\frac{i}{2\tau} \left(1 \mp \sqrt{1 - 4\tau D \mathbf{k}^2} \right). \quad (3)$$

The theory has two timescales: $\tau_{UV} \equiv -i/\omega_1$ is the timescale of the thermalization while $\tau_D \equiv -i/\omega_2$ is the diffusion time of the mode with momentum \mathbf{k} . For the long wavelength modes with $\tau \ll (D\mathbf{k}^2)^{-1}$:

$$\omega_1 = -iD\mathbf{k}^2, \quad \omega_2 = -\frac{i}{\tau} + iD\mathbf{k}^2, \quad (4)$$

which gives $\tau_D = (D\mathbf{k}^2)^{-1}$ and $\tau_{UV} = \tau$. This can be compared to Fick's law of diffusion, $\partial_t n - D\nabla^2 n = 0$, which encodes one single diffusion mode $\omega = -iD\mathbf{k}^2$. Since ω_2 is a UV mode for Fick's law, we refer to (2) as the (phenomenological) theory of diffusion, UV regulated with a physical gapped mode.

Our intent is to make Eq. (2) nonlinear. When n does not couple to any dynamical field, this is achieved by including the self-interactions of n [8]. These enter by promoting D to be a function of small fluctuations about $n = 0$: $D(n) = D + \lambda_D n + (\lambda'_D/2)n^2 + \dots$, where $\lambda_D = dD(n)/dn$, $\lambda'_D = d^2D(n)/dn^2, \dots$. Dropping terms with orders higher than 2, the nonlinear version of (2) is found to be

$$E[n] \equiv \tau \partial_t^2 n + \partial_t n - \nabla^2 \left(Dn + \frac{\lambda_D}{2} n^2 + \frac{\lambda'_D}{6} n^3 \right) = 0. \quad (5)$$

In general τ could be a function of \mathbf{J} in (1). However, since there is no other vector involved in the setup, the scalar τ cannot depend on the vector \mathbf{J} at linear order; the first contribution is quadratic in \mathbf{J} and turns out not to contribute to any of our results. We take τ constant in

what follows. Note also that if n refers to a charge density, then under its changing sign, $\lambda_D \rightarrow -\lambda_D$ but D and λ'_D remain the same.

Our goal is to study correlations between fluctuations of n . For this, we construct an effective action for n whose equation of motion is (5). We do this in the framework of MSR formalism [22]. The idea is to put a noise term on the right side of (5) and then impose the fluctuation-dissipation theorem to fix its strength. Finally, exponentiating this stochastic equation yields the effective action $S_{\text{eff}} = \int dt d^d x \mathcal{L}$. As we show in Supplemental Material [23], the effective action takes the form

$$\mathcal{L} = iT\sigma(n)(\nabla n_a)^2 - n_a(\tau \partial_t^2 n + \partial_t n - \nabla D(n)\nabla n) + \dots, \quad (6)$$

where the charge conductivity $\sigma(n) = \sigma + \lambda_\sigma n + (\lambda'_\sigma/2)n^2 + \dots$, is related to the diffusion constant D at the leading order in n by the Einstein relation $\sigma = \chi D$ via the charge susceptibility χ . To quartic order in fields this becomes

$$\begin{aligned} \mathcal{L} = & iT\sigma(\nabla n_a)^2 - n_a(\tau \partial_t^2 n + \partial_t n - D\nabla^2 n) \\ & + iT\chi\lambda_\sigma n(\nabla n_a)^2 + \frac{\lambda_D}{2} \nabla^2 n_a n^2 \\ & + \frac{1}{2} iT\chi\lambda'_\sigma n^2(\nabla n_a)^2 + \frac{\lambda'_D}{6} \nabla^2 n_a n^3. \end{aligned} \quad (7)$$

Here, n_a is an auxiliary field, analogous to the a field in the Schwinger-Keldysh framework [6]. In the limit $\tau = 0$, (7) reduces to the theory of diffusive fluctuations [6]. At $\tau \neq 0$, (7) defines our novel theory of nonlinear diffusion with a physical gapped mode.

In order to study the leading effects caused by the nonlinear terms in (5), we investigate the effect of one-loop corrections on the retarded Green's function in the EFT described by (7). At one-loop order, only cubic interactions in (7) contribute. This is why we dropped higher order terms when expanding $D(n)$ and $\sigma(n)$. Even λ'_D and λ'_σ are not needed.

Results.—The retarded Green's function at one loop can be parametrized by

$$G_{nn}^R(\omega, \mathbf{k}) = \frac{i(\sigma + \delta\sigma(\omega, \mathbf{k}))\mathbf{k}^2}{-i\tau\omega^2 + \omega + iD\mathbf{k}^2 + \Sigma(\omega, \mathbf{k})}. \quad (8)$$

The self-energy is given by

$$G_{nn_a}^{(0)} \Sigma G_{nn_a}^{(0)} = \text{---} \text{---} \text{---} \text{---} + \text{---} \text{---} \text{---} \text{---} \quad (9)$$

where from the first line in (7) we have $G_{nn}^{(0)} = (\omega + iD\mathbf{k}^2 - i\tau\omega^2)^{-1}$. Considering a hard momentum cutoff, we evaluate the loop integrals. The cutoff-dependent parts of Σ can be absorbed into the bare values of coefficients D and τ . The cutoff-independent parts turn out to be nonanalytic, that are given in $d = 1, 2, 3$ dimensions by

$$\Sigma_d(\omega, \mathbf{k}) = \alpha_d(\omega, \mathbf{k})(\tau D)^{(2-d)/2} \frac{T\chi}{D^2} \mathbf{k}^2 [f_{1d}\lambda_D^2 + f_{2d}\lambda_D\lambda_\sigma]. \quad (10)$$

Here and below, f_{id} are analytic functions of ω and \mathbf{k} . The nonanalyticity is encoded in

$$\alpha_d(\omega, \mathbf{k}) = \frac{(-F(\omega, \mathbf{k}))^{(d/2)-1}}{(16\pi)^{d/2}\Gamma(\frac{d}{2})} \begin{cases} i\pi & d \text{ odd,} \\ \log \frac{1}{F(\omega, \mathbf{k})} & d \text{ even,} \end{cases} \quad (11)$$

with $F(\omega, \mathbf{k}) = \{(1 - i\tau\omega)^2(D\mathbf{k}^2\tau - i\omega\tau(2 - i\tau\omega))/[D\mathbf{k}^2\tau + (1 - i\tau\omega)^2]\}$. Having found Σ , the next step is to calculate the loop correction to the numerator of $G_{nn}^{R(1)}$. Similarly, we find (see Supplemental Material [23])

$$\frac{\delta\sigma_d(\omega, \mathbf{k})}{\sigma} = \alpha_d(\omega, \mathbf{k})(\tau D)^{(2-d)/2} \frac{T\chi}{D^2} \mathbf{k}^2 [f_{3d}\lambda_D^2 + f_{4d}\lambda_D\lambda_\sigma]. \quad (12)$$

The two expressions (10) and (12) fully specify (8). Rewriting it in the form

$$G_{nn}^R(\omega, \mathbf{k}) = \frac{i\sigma\mathbf{k}^2}{-i(\tau + \delta\tau(\omega, \mathbf{k}))\omega^2 + \omega + i(D + \delta D(\omega, \mathbf{k}))\mathbf{k}^2} \quad (13)$$

we find that

$$\delta D(\omega, \mathbf{k}) = \frac{\lambda_D^2 T\chi}{4D^2} (-i\omega)(\tau D)^{\frac{2-d}{2}} \alpha_d(\omega, \mathbf{k}) \times (1 - i\tau\omega) \left(\frac{2 + D\mathbf{k}^2\tau - \tau\omega(3i + \tau\omega)}{-D\mathbf{k}^2\tau + (i + \tau\omega)^2} \right)^2, \quad (14)$$

and $\delta\tau(\omega, \mathbf{k}) = 0$. The latter answers the first question raised in the Introduction: our theory, Eq. (7), predicts that the bound on local thermalization time τ (and thus the onset of diffusion) [14] is protected from renormalization caused by the fluctuations. In the Discussion, we show that this result is supported by the experimental data associated with the bad metallic system of [13]. Note that at $\tau = 0$, (14) reduces to the results found in [6,7].

Causality implies that G^R is analytic in the upper half of the complex frequency plane. However, the structure of

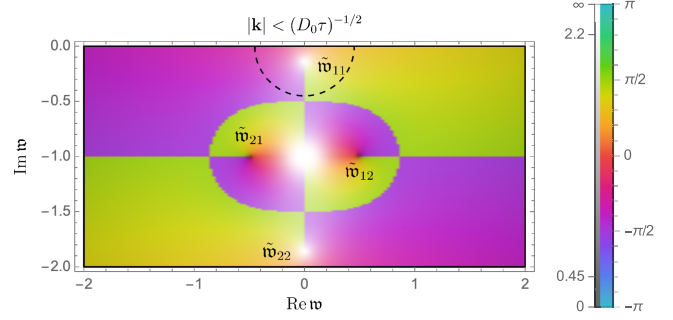


FIG. 1. Contour plot of the phase angle φ of the complex-valued $\alpha_1 = |\alpha_1| e^{i\varphi}$. Any discontinuous transition between two distinct colors represents a branch cut of the retarded Green's function in the complex $\mathfrak{w} = \omega\tau$ plane. For comparison, we have schematically illustrated the range accessible to the diffusive theory of Ref. [6] by a dashed semicircle in the top panel, while our theory of nonlinear diffusion (UV regulated) with a physical gapped mode is valid in the entire range displayed.

$F(\omega, \mathbf{k})$ indicates that, due to the interactions, four branch point singularities are induced in the lower half plane (Fig. 1):

$$\begin{aligned} \tilde{w}_{11,22} &= -\frac{i}{\tau} \left(1 \mp \sqrt{1 - D\mathbf{k}^2\tau} \right), \\ \tilde{w}_{12,21} &= -\frac{i}{\tau} \pm |\mathbf{k}| \sqrt{\frac{D}{\tau}}. \end{aligned} \quad (15)$$

These branch points correspond to the minimum energy for generating two on-shell excitations with the dispersion (3) in the loops, as explained in Supplemental Material [23]. The location of branch points will be important when finding the inverse Fourier transform of momentum space correlation functions.

As the last formal result, we find $\mathfrak{G}_{nn}(t, \mathbf{k}) = \int (d\omega/2\pi) G_{nn}(\omega, \mathbf{k}) e^{-i\omega t}$. Note that $G_{nn}(\omega, \mathbf{k})$ can be simply calculated from $G_{nn}^R(\omega, \mathbf{k})$ via the fluctuation-dissipation theorem. While at $\tau = 0$ one finds $\mathfrak{G}_{nn}(t, \mathbf{k})$ analytically [38], at $\tau \neq 0$ we were not able to represent $\mathfrak{G}_{nn}(t, \mathbf{k})$ in terms of known special functions. Thus, we find this function numerically.

The results for $\lambda_{\text{eff}}^2 \equiv [T\chi/(\tau D^5)^{1/2}] \lambda_D^2 = \frac{1}{2}$ are displayed in Fig. 2. For $t \gg \tau_D$, $r = \tau_{UV}/\tau_D$ has no significant effect; the two solid line curves converge similarly. However, the effect of r is significant at $t \ll \tau_D$. As shown in the inset, for $r = (1/10)$, the correlation function around $t = (1/10)\tau_D$ decays slower than for $r = (1/100)$. This is related to the second branch point in Fig. 1, i.e., \tilde{w}_{22} . As mentioned earlier, we did not find \mathfrak{G}_{nn} analytically; but one would expect that when evaluating the Fourier integral, among other contributions, picking up the pole \tilde{w}_{22} would yield a term $\propto e^{-i\tilde{w}_{22}t} \sim e^{-t/\tau_{UV}}$. This would give a finite contribution at $t \lesssim \tau_{UV} \sim r\tau_D$, which justifies the excess shown in the inset. Obviously, when $\tau_{UV} \rightarrow 0$ [6,7],

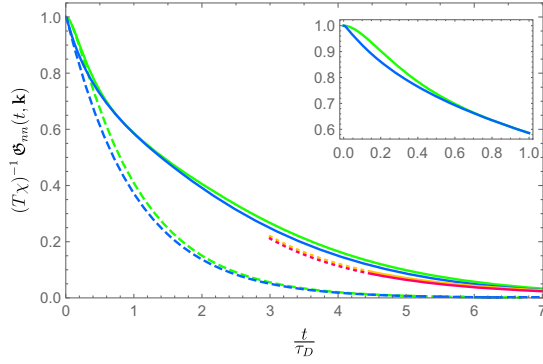


FIG. 2. Solid blue and green curves show $\mathfrak{G}_{nn}^{(0)+(1)}$ while dashed curves correspond to $\mathfrak{G}_{nn}^{(0)}$. With blue and green, we illustrate distinct values of $r = \tau_{UV}/\tau_D$: 1/100 and 1/10, respectively. The red and yellow curves show the longtime tail of $\mathfrak{G}_{nn}^{(0)+(1)}$ for these two values of r .

\tilde{w}_{22} becomes $-i\infty$, so the effect disappears. We emphasize that this feature is valid in static systems. In a dynamical background, the perturbations may not decay solely by an exponential term [39].

In the limit $\tau_D \ll t$, we find the asymptotic behavior of $\mathfrak{G}_{nn}^{(1)}(t, \mathbf{k})$ analytically. This “longtime tail,” illustrated in red ($r = (1/10)$) and yellow ($r = (1/100)$) in Fig. 2, comes from integration over the region surrounded by the dashed semicircle in Fig. 1. For $t > 0$ and $d = 1$:

$$\mathfrak{G}_{nn}^{(1)}(t, \mathbf{k}) = g \frac{(1 + \sqrt{1 - \tau D \mathbf{k}^2})^4}{(1 - \tau D \mathbf{k}^2)^{1/4}} \frac{e^{(-1 + \sqrt{1 - \tau D \mathbf{k}^2})t}}{\sqrt{2\pi D t}}, \quad (16)$$

where $g = (\lambda_D^2/16D^2)T^2\chi^2$. This answers the second question raised in the Introduction: the fast thermalization of the nonconserved current \mathbf{J} does not affect the fractional power of the longtime tail. We find $t^{-1/2}$, which is identical to the known behavior $t^{-d/2}$ without UV regulator [10]. But the exponential decay associated with diffusive fluctuations changes. When $\tau = 0$, the late-time behavior is given by $e^{-\frac{1}{2}D\mathbf{k}^2 t}$ [40]. The effect of the gapped mode is to decrease this factor at any \mathbf{k} . We emphasize that this exponential decay is specific to static systems near equilibrium. See Ref. [39] for a discussion on the existence of late-time universal attractors in a longitudinally expanding QGP.

Applications and discussion.—Bad metal: Let us check the results of our theory against data from the bad metallic system [13] mentioned in the Introduction. In [13], the charge density $n(t, \mathbf{k})$ is identified with twice the experimentally measured atomic density of one spin component. The data from [13] consist of eight groups of points, each group of points contains ten $n(t, \mathbf{k})$ values, with a fixed value of \mathbf{k} . Reference [13] fits the data using the *analytical* solution of (2) to determine Γ , D and $\delta n \equiv n(0, \mathbf{k})$. However, at high temperatures, which is

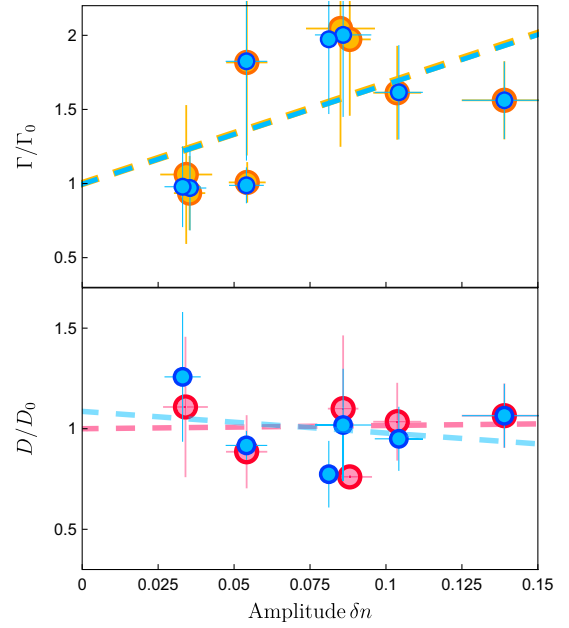


FIG. 3. Variation of fitting parameters Γ (top), D (bottom) versus the amplitude of the solution, namely $n(0, \mathbf{k})$. Orange and red dots are obtained by fitting the data of [13] to the linear Eq. (2) while blue dots stem from fitting the data to the nonlinear Eq. (5). The orange, red, and blue dashed lines are the corresponding linear fits. Γ and D are normalized by the extrapolated zero-amplitude values Γ_0 and D_0 , respectively. Error bars indicate the standard error of the mean value resulting from our fits.

the case in [13], the thermalization length becomes short, on the order of the lattice spacing, and fluctuation corrections are of order one [6]. Therefore, instead of fitting data to the linear equation (2), as done in [13], we propose the nonlinear equation (5). Figure 3 illustrates the results of this fit (blue) compared to the results of the linear equation fit (orange and red). For the sake of consistency, in both cases we fit data with the *numerical* solution of the equation. For the linear case we find three parameters as in [13], while in the nonlinear case we also find a fourth parameter: λ_D . Our nonlinear fit procedure and the dependence of our results on it are detailed step by step in Supplemental Material [23].

As shown in the top panel, the linear fit of blue dots (blue line) is coincident with the linear fit of orange dots (orange line). Since each pair of orange-blue dots is associated with a specific \mathbf{k} , this coincidence implies $\delta\Gamma(\mathbf{k}) \approx 0$. This may be regarded as the realization of our earlier statement that $\tau = \Gamma^{-1}$ is protected from the nonlinear corrections in our model.

The bottom panel of Fig. 3 indicates that $\delta D(\mathbf{k})$ is nonzero for almost all values of \mathbf{k} in the experiment of [13]. In other words, the diffusion constant is significantly renormalized by nonlinear effects. This is in agreement with the prediction of our theory.

As pointed out in [13], their fit of large-initial-amplitude data with the linear equation is merely an attempt to evaluate the possibility of nonlinear effects. We now see from Fig. 3 that the data are also consistent with our nonlinear equation (5). From Fig. 3 and with the data currently available to us, it is not possible to judge if the nonlinear fit is a better fit to the data. However, based on [6], we can assume that large fluctuations exist in the system and thus nonlinearities must be taken into account. Therefore, our nonlinear fit is preferred to the linear fit from [13], having at least two quantitative advantages: First, the value of D obtained here is more reliable than that of [13]. Second, the value of $\lambda_D = dD(n)/dn$ can only be extracted from the nonlinear fit of the data (see Supplemental Material [23]).

Bjorken expansion: A simple dynamical system to study the effect of a UV regulator on diffusive fluctuations is the Bjorken flow, which is a hydrodynamic model for the longitudinal expansion of the QGP.

The effect of nonlinear fluctuations in Bjorken flow has been studied in Ref. [41]. Developing a set of hydrokinetic equations, the first fractional power correction to the longitudinal pressure at late times was found as $\propto 1/(\tau_p T)^{3/2}$ (τ_p is the proper time and $1/\tau_p$ the expansion rate of the Bjorken flow). If the expanding flow has a U(1) charge, the fluctuations also result in a fractional power correction of the U(1) current. This is the consequence of nonlinear mode coupling between the currents and the hydrodynamic variables [42]. In contrast to previous studies, our model also features a UV regulator, i.e., τ . Without deriving hydrokinetic equations, we estimate the effect of the UV regulator on the late-time nonlinear correction to the single charge density, $\Delta\langle n(\tau_p) \rangle$, in “nonfluctuating” Bjorken flow. In contrast to [42], the effect comes from the self-interactions of n . We find (Supplemental Material [23])

$$\Delta\langle n(\tau_p) \rangle = aT\chi^2\mu \frac{\lambda_D^2}{D^2} \frac{1}{(D\tau_p)^{3/2}} \left(1 - \frac{11}{8} \frac{\tau}{\tau_p} + \dots \right). \quad (17)$$

The leading correction is similar to Eq. (78a) in [42]. In fact this term can be found through the work of [6,7]. However, the subleading term is found entirely from the theory proposed in this Letter, representing the effect of the UV regulator. This is important, but if $\tau \ll \tau_p$ it will be smaller than the leading non-linear effects. In order to make the above results more accurate in a more realistic scenario, it would be interesting to investigate the effect of the UV regulator on the hydrokinetic setup of [42].

Another aspect of our theory of nonlinear diffusion, worthy of future exploration, is its application near a critical point, such as, for example, the critical point expected in the QCD phase diagram. Near such critical point charge fluctuations, the correlation length, and the relaxation time of our UV mode all become large [43], such that it has to be

included into the long-wavelength description [44], making our nonlinear theory of diffusion relevant to the search for the critical point [45–47]; see Supplemental Material [23].

We thank P. Kovtun and A. Davody for helpful discussions. For comments on the draft we thank L. Delacrétaz, P. Glorioso, and E. van Heumen. M. K. was supported, in part, by the U.S. Department of Energy Grant No. DE-SC0012447. M. K. thanks the Universität Würzburg and the APCTP where part of this work was carried out. N. A. was supported by Grant No. 561119208 “Double First Class” start-up funding of Lanzhou University, China.

*abbasi@lzu.edu.cn

†mski@ua.edu

‡otavakol@physics.utoronto.ca

- [1] M. Crossley, P. Glorioso, and H. Liu, *J. High Energy Phys.* **09** (2017) 095.
- [2] K. Jensen, R. Marjeh, N. Pinzani-Fokeeva, and A. Yarom, *SciPost Phys.* **5**, 053 (2018).
- [3] F. M. Haehl, R. Loganayagam, and M. Rangamani, *J. High Energy Phys.* **05** (2015) 060.
- [4] H. Liu and P. Glorioso, *Proc. Sci., TASI2017* (2018) 008 [arXiv:1805.09331].
- [5] This was discussed in [6–8]. While [6] focuses on density fluctuations in the framework of Schwinger-Keldysh, [7] studies multiplicative noise, arisen from such nonlinear dependence in the context of stochastic fluid dynamics. See also [9].
- [6] X. Chen-Lin, L. V. Delacrétaz, and S. A. Hartnoll, *Phys. Rev. Lett.* **122**, 091602 (2019).
- [7] J. Chao and T. Schaefer, *J. High Energy Phys.* **01** (2021) 071.
- [8] P. Kovtun, *J. Phys. A* **48**, 265002 (2015).
- [9] J. Chao and T. Schaefer, *J. High Energy Phys.* **06** (2023) 057.
- [10] P. Kovtun and L. G. Yaffe, *Phys. Rev. D* **68**, 025007 (2003).
- [11] P. Kovtun, G. D. Moore, and P. Romatschke, *Phys. Rev. D* **84**, 025006 (2011).
- [12] L. P. Kadanoff and P. C. Martin, *Ann. Phys. (N.Y.)* **24**, 419 (1963).
- [13] P. T. Brown *et al.*, *Science* **363**, 379 (2019).
- [14] S. A. Hartnoll and A. P. Mackenzie, *Rev. Mod. Phys.* **94**, 041002 (2022).
- [15] When the system is not static, flow dependent timescales are also involved in thermalization. Examples are the weakly coupled system of [16] under the Bjorken flow, and [17] under the FLRW expansion.
- [16] A. Behtash, S. Kamata, M. Martinez, and H. Shi, *Phys. Rev. D* **99**, 116012 (2019).
- [17] D. Bazow, G. S. Denicol, U. Heinz, M. Martinez, and J. Noronha, *Phys. Rev. Lett.* **116**, 022301 (2016).
- [18] M. H. Ernst, E. H. Hauge, and J. M. J. van Leeuwen, *Phys. Rev. Lett.* **25**, 1254 (1970).
- [19] B. J. Alder and T. E. Wainwright, *Phys. Rev. A* **1**, 18 (1970).
- [20] We focus on static systems. Systems in a dynamical background may not exhibit such exponential behavior; for example, the Gubser flow [21].

- [21] S. S. Gubser, *Phys. Rev. D* **82**, 085027 (2010).
- [22] P. C. Martin, E. D. Siggia, and H. A. Rose, *Phys. Rev. A* **8**, 423 (1973).
- [23] See Supplemental Material at <http://link.aps.org/supplemental/10.1103/PhysRevLett.132.131602> for details on correlation functions, microscopic fluctuations, the effective action, loop calculations, threshold singularities, dispersion relations, long time tails, the effect of the UV regulator on fluctuations in expanding QGP, the fitting method comparing to Ref. [11], and application of our theory near a critical point, which includes Refs. [24–37].
- [24] L. D. Landau and E. M. Lifshitz, *Statistical Physics, Part I*, 3rd ed. (Pergamon Press, Oxford, 1980), Vol. 5.
- [25] L. V. Delacretaz, A. L. Fitzpatrick, E. Katz, and M. T. Walters, *J. High Energy Phys.* **02** (2023) 045.
- [26] P. Romatschke and U. Romatschke, *Relativistic Fluid Dynamics In and Out of Equilibrium* (Cambridge University Press, Cambridge, England, 2019).
- [27] P. Kovtun, *J. Phys. A* **45**, 473001 (2012).
- [28] N. Abbasi, *J. High Energy Phys.* **04** (2022) 181.
- [29] E. Wang and U. W. Heinz, *Phys. Rev. D* **66**, 025008 (2002).
- [30] M. Baggioli and M. Landry, *SciPost Phys.* **9**, 062 (2020).
- [31] L. V. Delacrétaz, B. Goutéraux, and V. Ziogas, *Phys. Rev. Lett.* **128**, 141601 (2022).
- [32] W. Israel and J. M. Stewart, *Ann. Phys. (N.Y.)* **118**, 341 (1979).
- [33] I. Müller, *Z. Phys.* **198**, 329 (1967).
- [34] W. Israel, *Ann. Phys. (N.Y.)* **100**, 310 (1976).
- [35] S. Jeon and U. Heinz, *Int. J. Mod. Phys. E* **24**, 1530010 (2015).
- [36] C. Gale, S. Jeon, and B. Schenke, *Int. J. Mod. Phys. A* **28**, 1340011 (2013).
- [37] L. Du, X. An, and U. Heinz, *Phys. Rev. C* **104**, 064904 (2021).
- [38] A. A. Michailidis, D. A. Abanin, and L. V. Delacrétaz, [arXiv:2310.10564](https://arxiv.org/abs/2310.10564).
- [39] M. P. Heller and M. Spalinski, *Phys. Rev. Lett.* **115**, 072501 (2015).
- [40] L. V. Delacretaz, *SciPost Phys.* **9**, 034 (2020).
- [41] Y. Akamatsu, A. Mazeliauskas, and D. Teaney, *Phys. Rev. C* **95**, 014909 (2017).
- [42] M. Martinez and T. Schäfer, *Phys. Rev. C* **99**, 054902 (2019).
- [43] P. C. Hohenberg and B. I. Halperin, *Rev. Mod. Phys.* **49**, 435 (1977).
- [44] M. Stephanov and Y. Yin, *Phys. Rev. D* **98**, 036006 (2018).
- [45] M. A. Stephanov, K. Rajagopal, and E. V. Shuryak, *Phys. Rev. Lett.* **81**, 4816 (1998).
- [46] L. Du, U. Heinz, K. Rajagopal, and Y. Yin, *Phys. Rev. C* **102**, 054911 (2020).
- [47] M. A. Stephanov, *Phys. Rev. Lett.* **102**, 032301 (2009).